DAPNIA-SEA-93-14

C.E. SACLAY
DSM

SERVICE D'ÉTUDE DES ACCÉLÉRATEURS

Fermilab Library
0 1160 0027991 3

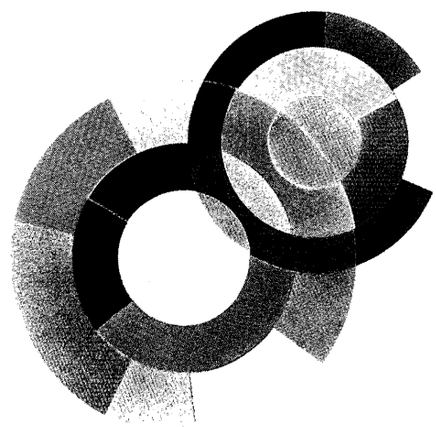

DAPNIA/SEA 93 14 10/1993

STUDY OF MICROWAVE FIELD EMISSION

J. Tan, H. Safa, B. Bonin, M. Jimenez,
J.M. Tessier

DAPNIA

Couverture : Sylvie Cobrit et Marc Souvage

Le DAPNIA (**D**épartement d'**A**strophysique, de physique des **P**articules, de physique **N**ucléaire et de l'**I**nstrumentation **A**ssociée) regroupe les activités du Service d'Astrophysique (SAp), du Département de Physique des Particules Elémentaires (DPhPE) et du Département de Physique Nucléaire (DPhN).

Adresse : DAPNIA, Bâtiment 141
CEA Saclay
F - 91191 Gif-sur-Yvette Cedex

Soumis pour publication dans :

Journal of Applied Physics D

STUDY OF MICROWAVE FIELD EMISSION

J. Tan

Thomson Tubes Electroniques, 78140 Vélizy, France

H. Safa, B. Bonin, M. Jimenez, J.-M. Tessier

C.E. Saclay, 91191 Gif-sur-Yvette, France

Abstract

We have developped an apparatus to measure directly on samples the current produced by field emission in a 1.5 GHz cavity. After giving details of the experiment design, we review all observations seen during our measurements. Then, we briefly summarize the main results obtained compiling about a hundred tests done up to now. Finally, some follow-up that could be done in a the near future is suggested.

I – Aim of the experiment

When submitted to an intense electric field, a metallic surface in vacuum generally exhibits electronic emission. This phenomenon, known as enhanced field emission [1], is a precursor to breakdown which affects the behaviour of many devices (electron guns, klystrons, vacuum switches, cavities for accelerators, etc...). Till now, a great research effort has been devoted to the study of field emission (FE) in a steady (DC) electric field. The question of the influence of the frequency is not yet clear: Is the field emission in a radiofrequency (RF) field the same as in a continuous one? In order to study the basic physics behind this phenomenon, we were led to build a cavity in which we were able to produce locally on a removable sample a strong enough RF electric field as compared to the other parts of the cavity. In that way, we ensure that if emission has to happen, it has a much greater chance to come from the sample. Moreover, we would like to measure directly the current emitted when it occurs and then compare it to the DC field emission obtained on the *same* sample on other apparatus we already have at Saclay [2,3]. Finally this experiment would be used to study the influence of various surface treatments on FE —for the purpose of reducing or enhancing it — as well as to understand its causes ("dust" particles, scratches, adsorbed gases, oxide layers, etc...).

II – The RF cavity

1– Design

To start with, we intended to use as the RF power source a THOMSON TH2466 klystron which delivers 5kW of continuous output power and is centered at 1495MHz with 10MHz bandwidth. These two parameters (maximum available power and fixed frequency) will determine the cavity geometry as we will see it later on. The other fundamental choice was to work at room temperature [4,5] as compared to having a superconducting cavity (see for instance U. Klein's resonator [6] or the special TM020 mode cavity of Cornell [7]). Theoretically, the temperature in itself should have a very small effect on the field emission: the profile change in the density of states when the temperature rises from T=0K to T=300K should lead to an increase of barely a few percent in the emitted current even for fields as high as 10^9V/m. Neither should the superconducting state affect FE [8]. The enormous simplification resulting from getting rid of all the cryogenics together with the much faster turnover of the measurements (typically 3 per day instead of one a week) were convincing advantages. The only drawback was the lower fields obtained for a given power. This had to be compensated by a local enhancement of the field at the position of the sample. We aimed at getting at least 50MV/m for the 5kW available. Thus, we must maximize the ratio $E_p/\sqrt{P_d}$, where E_p is the peak electric RF field and P_d the dissipated power in the cavity. The (λ/4) resonator cavity scheme (figure 1) appeared likely to suit this purpose because the electric field is concentrated at the vicinity of the cavity nose [9]. Actually, the so called

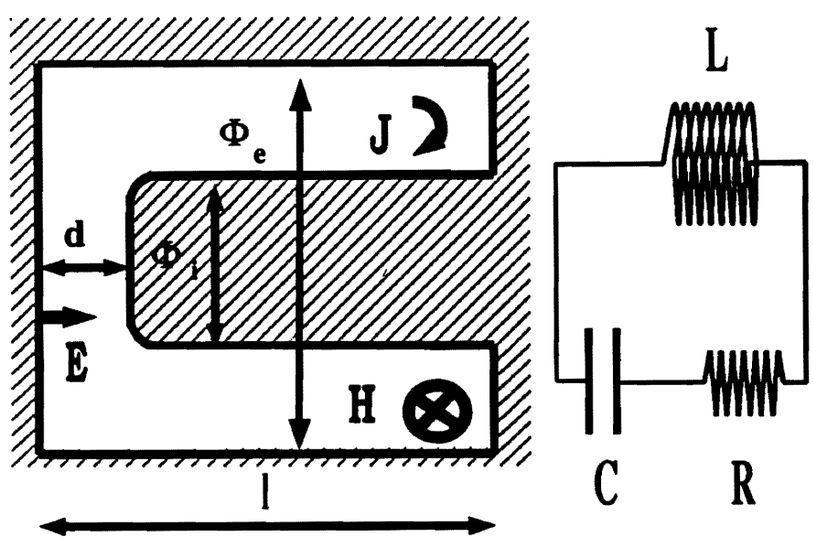

Figure 1– A (λ/4)– Resonator

re-entrant cavity can be approximated with a very simple lumped elements circuit containing a capacitor C and an inductor L having the values $L = \frac{\eta}{2\pi\omega\sqrt{\epsilon_r}} Log\left(\frac{\Phi_e}{\Phi_i}\right) \tan\left(\frac{\omega l\sqrt{\epsilon_r}}{c}\right)$, $C = \frac{\epsilon\pi\Phi_i^2}{4d}$, η=377Ω being the vacuum impedance, ω the angular frequency, ϵ_r the relative permittivity and ϵ the total permittivity of the medium, c the speed of light and the other geometrical parameters as shown on the figure, Φ_i and Φ_e denoting the inner and outer diameters, l the overall length and d the small gap. The resonances are given by the condition $LC\omega^2 = 1$, which indicates that $l \lesssim (2n+1)\left(\frac{\lambda}{4}\right)$, $(n \ integer)$ justifying the naming of the resonator as the first resonance is close to (λ/4). Our above ratio can be rewritten as $\left(\frac{R}{Q}\right) = \frac{1}{C\omega} = \frac{\eta}{2\pi\sqrt{\epsilon_r}} Log\left(\frac{\Phi_e}{\Phi_i}\right) \tan\left(\frac{\omega l\sqrt{\epsilon_r}}{c}\right)$ indicating that the only way to increase our coefficient is to increase the ratio $\frac{\Phi_e}{\Phi_i}$. But this means having a small sample diameter. Moreover, the smaller the sample diameter, the more sensitive is the resonance frequency to mechanical tolerances. We had then to compromise between a high $\left(E_p/\sqrt{P_d}\right)$ on the one hand and a large enough sample area and acceptable mechanical tolerances to stay inside the klystron bandwidth on the other. This led us to choose a value of Φ_i=3mm with a hemispherical end in order not to introduce any sharp angle that might induce uncontrolled high electric fields. As the shape was defined, a more precise calculation of the electromagnetic fields in the cavity was done using the 2–D code URMEL [10]. The results were a theoretical Q_0 of the cavity of 10600, assuming that all the surfaces including the sample are pure OFHC copper. From the calculation, one can also deduce the ratio $\left(E_p/\sqrt{P_d}\right) = 1.09 \ (MV/m)/\sqrt{W}$ which assures a maximum field of 68.9MV/m for 4kW of dissipated power in the cavity.

2– RF couplings and current antenna

One would like to get a critical input coupling (β=1) in order to minimise return loss (VSWR) and to save power, whereas the transmitted coupling should be low ($\beta\sim$0.01). All RF feedthroughs have been realized with 50Ω sealed N-connectors ensuring vacuum tightness. They are terminated by antennas plunging down into the cavity. Coupling is then capacitively induced by the electric field at the surface of the antennas. N-type connectors have been chosen as they can withstand 5kW of peak power without any damage and are conveniently small and easy to change if any trouble occurs (for higher power, one should switch to a waveguide input). Moreover, the cavity can then be easily moved around as the connection with the output of the klystron is merely a flexible N-cable.

The current antenna is a probe where the emission current produced by the electrons hitting the surface can be measured. It should have a very good DC isolation (>10^{14}Ω) but in RF on the contrary show a low equivalent impedance (ideally a short circuit). This can be realized with a λ/4 transformer from the standard 50Ω characteristic impedance to a low impedance. The total impedance seen from the cavity is $Z = \frac{Z_2^2}{Z_1} = 0.3\Omega$. The diameter and length of the antenna will determine the fraction of the sample from where emitters can be detected. If the antenna goes close to the sample, a wider area will be covered as electrons could be collected from emitter sites lying farther from the center. But if it gets too close, then the RF field on the antenna will be important and likely to begin having electrons

emitted from the antenna. A distance of D=12mm between the top of the sample and the

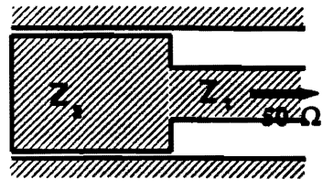

Figure 2– Antenna Transformer

antenna was chosen. For this value, the maximum field at the antenna is then only 2.4% of the peak field and that should be safe for not having electron emission *from* the antenna. Further, the total RF power dissipated in the $\lambda/4$ transformer is less than 0.05%, meaning that it loses only 2W out of a total of 4kW in the cavity. It seemed very convenient to use the same N-type feedthrough as those of the RF couplers followed by a (N-BNC) transition to extract the average DC current.

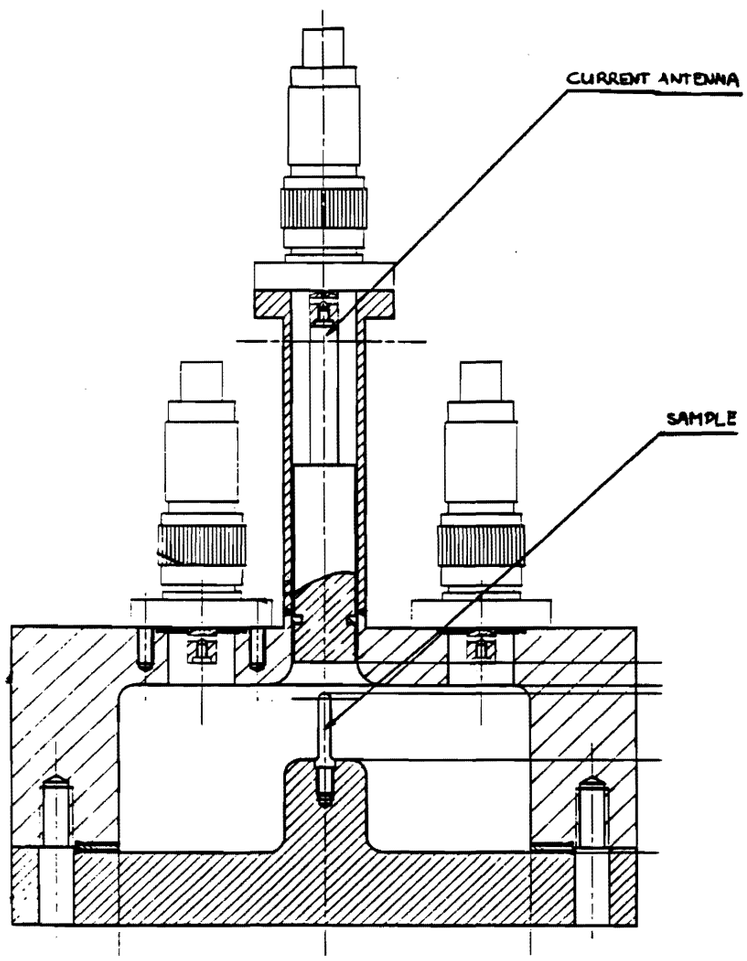

Figure 3– General Sketch of the cavity

3– Low power RF measurements

These RF measurements are done using an HP network analyser. The first thing is to check the resonance frequency which should be around 1495MHz. It should be noted that the sensitivity of the frequency f to the geometrical parameters is large. The main variation concern the sample diameter Φ_i and the gap d. We have $\frac{\partial f}{\partial d} = -\frac{\partial f}{\partial \Phi_i} = 40\ MHz/mm$.

Couplings Measuring the S-parameters of the cavity, and the loaded Q_l, we can deduce the external Q of either the input or the transmitted coupler. In figure 4, the value of Q_{ext} is plotted while varying the depth of the antenna inside the cavity (the z=0 or reference plane is taken to be the inner cavity surface as with the gap definition). It should also be noted that these Q's exactly correspond to what can be calculated from the position of the couplers, the electrical field E at that position and the antenna diameter Φ_a by assuming that the induced current in the coupler is the displacement current. This leads to

$$Q_{ext} = \frac{2\ W}{\epsilon^2 \omega Z_c E^2 S^2}$$

W beeing the total electromagnetic energy in the cavity, $S = \pi \Phi_a^2/4$ the surface of the antenna, and Z_c the characteristic impedance of the coupler line — 50Ω in our case. Choosing the

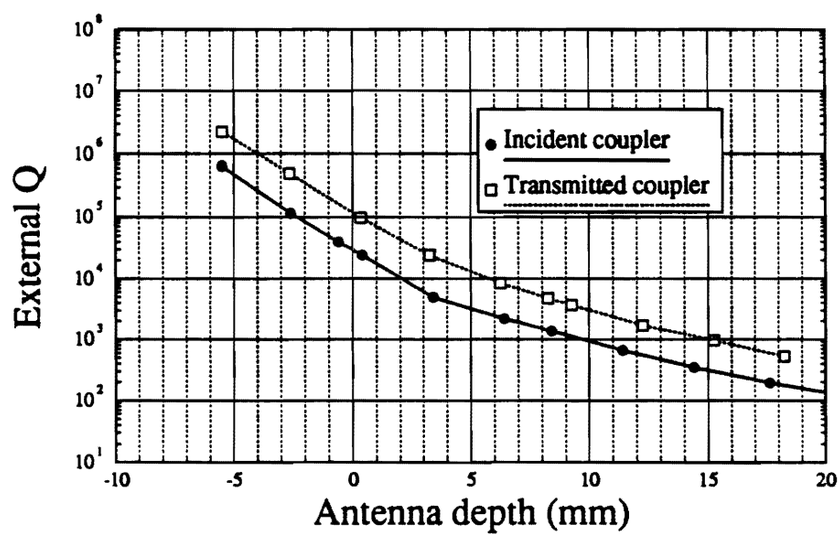

Figure 4– External Q as a function of the depth of the antenna

lengths for the antennas in order to obtain the desired couplings, one can measure typically

using a copper sample the following values :

$$Q_i = 7000$$
$$Q_t = 350000$$
$$Q_{current\ antenna} = 80000$$
$$(when\ not\ short - circuited)$$
$$Q_0 = 8600$$

One would always expect a value of Q_0 less than the theoretical one as "real" surfaces are worse than "ideal" ones (for example, surface roughness may contribute to increase the apparent surface resistance). Anyway, in our case, getting 80% of the theoretical Q_0 decreases the $(E_p/\sqrt{P_d})$ ratio to roughly 0.90 $(MV/m)/\sqrt{W}$. Moreover, with a niobium sample for instance, the Q_0 dropped to around 6000 (the surface resistance of niobium is 3 times that of copper) thus reducing even more the maximum field in the cavity. On the other hand, it is possible to immerse the cavity in a vessel filled with liquid nitrogen. At the temperature T=77K, an enhancement of Q_0 by a factor of 1.66 is measured enabling us to go even higher. The following table shows the maximum field one can obtain with 4 kW of dissipated power in the cavity.

Sample	Q_0	$(E_p/\sqrt{P_d})$ $(MV/m)/\sqrt{W}$	E_p (MV/m)
Theoretical copper	10600	1.09	68.9
Experimental copper T=300K	8600	0.98	62.1
Niobium (T=300K)	6000	0.82	51.9
Niobium (T=77K)	10000	1.06	67.0
Copper (T=77K)	16600	1.36	86.3

Table 1– Maximum electric field attainable

Check of the RF electric field We used the perturbation method [11,12] to measure experimentally the electric field strength along the axis for a given amount of power into the cavity. We adapted an apparatus which has been developped in our laboratory [13]. The current antenna was removed and replaced by a cup with a small hole pierced in it. A small metallic needle (length 0.75mm and diameter 0.45mm) has been chosen as the perturbating object and attached to a thread crossing the cavity (see figure 5). The principle is to measure the variation of the resonance frequency as the object goes along the axis. The relative

frequency shift due to the perturbation is [14] :

$$\frac{\Delta f}{f} = \frac{\int_v (\mu H^2 - \epsilon E^2)}{\int_V (\mu H^2 + \epsilon E^2)}$$

where v is the volume of the object, V the cavity volume, E and H the electric and magnetic fields and the ϵ and μ's the standard notations for the permittivity and permeability. Correcting for the finite length and shape of the perturbating object, one can evaluate the average electric field it sees.

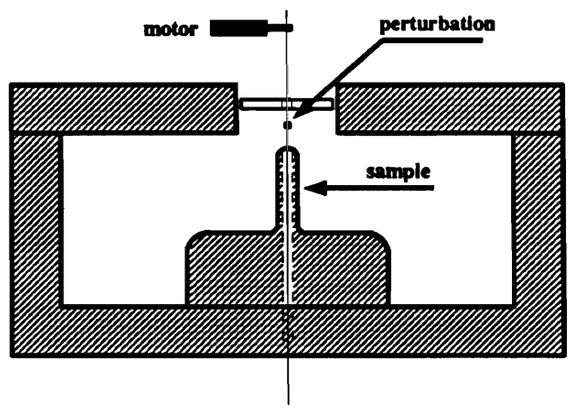

Figure 5– Experimental set for field measurement by perturbation method

The comparison between this measured field and the one calculated from the electromagnetic computer code is shown in figure 6. As can be seen, the matching is quite satisfactory and confirm that the real macroscopic RF field in the cavity has been correctly evaluated.

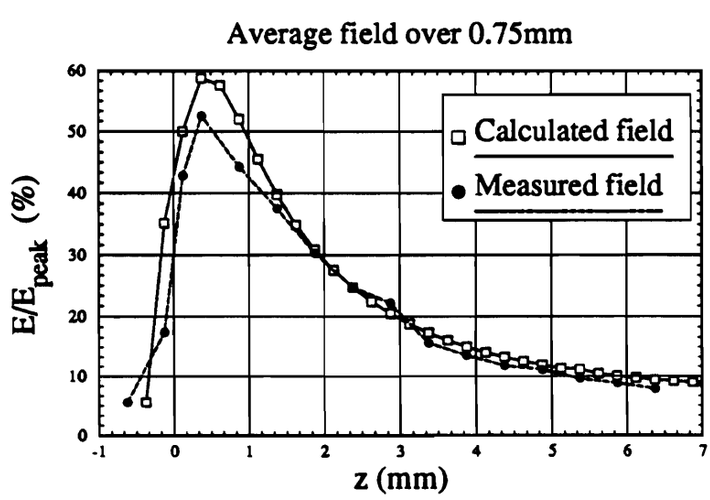

Figure 6– Comparison between calculated and measured electromagnetic field averaged over the needle's length

4– Electron trajectories and impact energy

The electric field is normal to the surface of the sample, where it can be considered as nearly constant (figure 7). But it decreases very rapidly (almost exponentially) as the

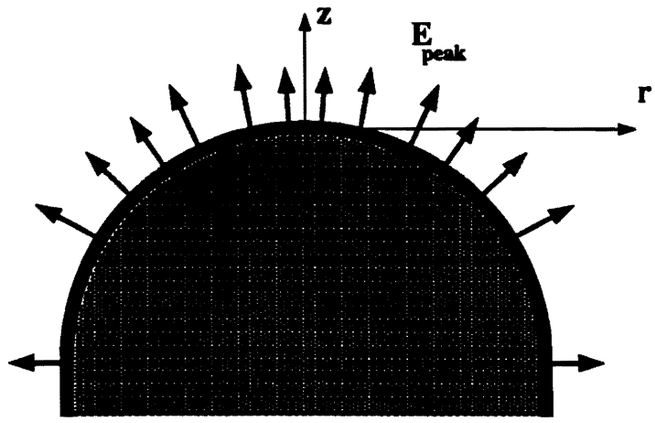

Figure 7– Field along the hemispherical surface of the sample. Strength is proportionnal to the length of the arrow.

distance to the surface increases. This behaviour is significant because it ensures that no FE will occur from unexpected places in the cavity, especially not from the current collecting antenna (figure 8).

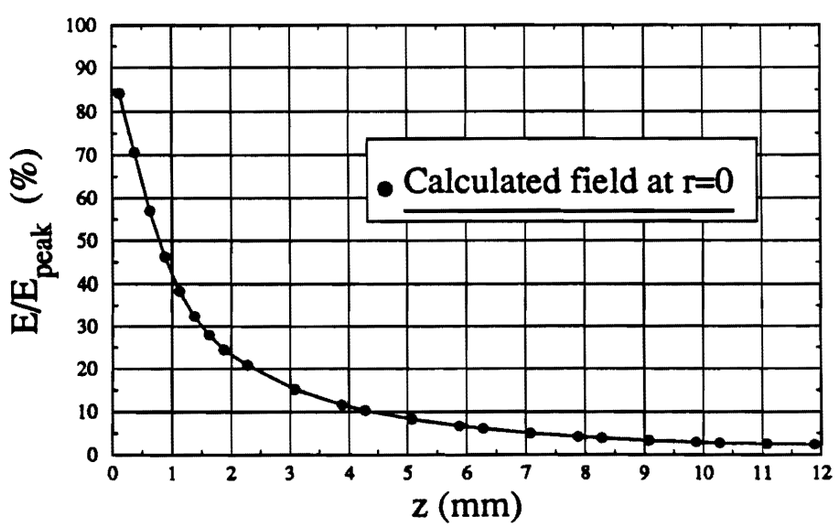

Figure 8– Relative field strength along the r=0 axis starting from the top of the sample. We see that the field at the antenna is only a few percent of peak field.

Another important consequence is that the electron trajectories starting from the sample are almost straight lines perpendicular to the sample surface (figure 9).

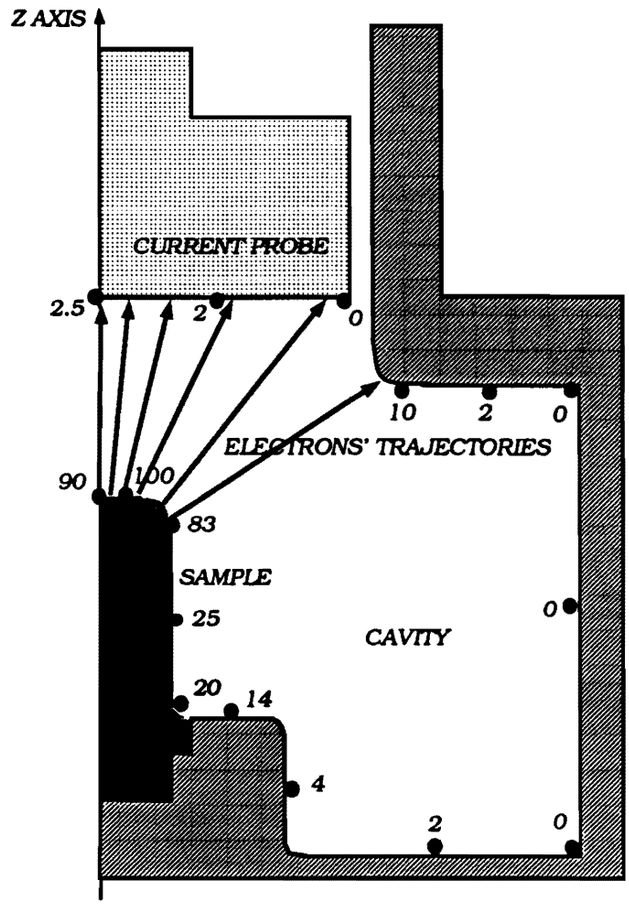

Figure 9– Trajectories followed by the emitted electrons. The value of field in percentage of peak field is indicated in some points of the cavity.

What can be also seen is that at the distance we have chosen to put the current antenna (12mm from the sample), only the electrons emitted from an emitting site lying within a 1.5mm diameter around the center will be collected by the current antenna. Other emitting sites may exist but will not be measured. This is another reason to have a large current antenna facing the sample. Knowing the field all along the trajectory, one can also calculate the electron energy as a function of time — or distance from the sample — and thus its final energy when it hits the current antenna (assuming that it leaves the sample with practically no initial velocity — a few eV —). All the energy taken from the RF field is at the very beginning (the first two millimeters) and then the electrons have enough energy to follow straight trajectories. The transit time between the emitter and the collecting antenna is quite

small compared to the RF period for electric fields higher than 3MV/m so one need not fear any backstream on the sample. Figure 10 shows both the transit time and the impact energy of the electrons as a function of the peak electric field. This will be useful later on for comparison with the X-ray measurements.

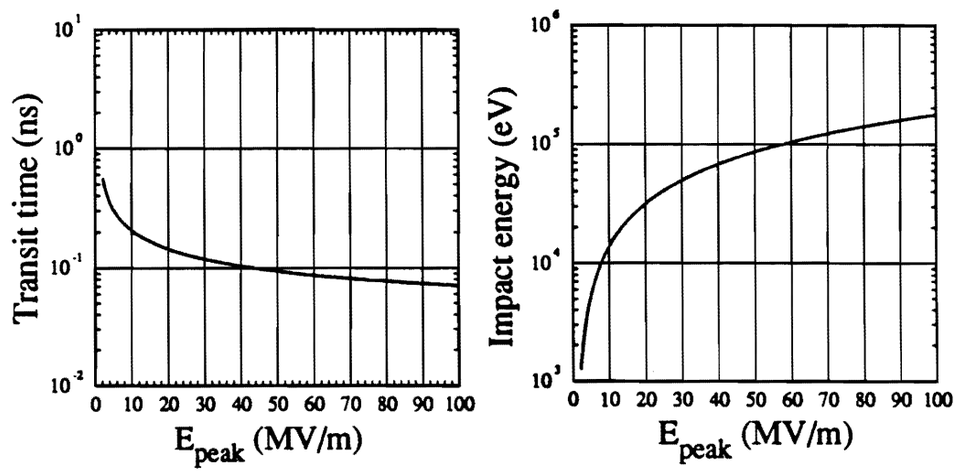

Figure 10– Transit time and final energy of emitted electrons

III – Experimental set-up

The experimental apparatus can be divided in 3 major blocks : The RF portion, the emission current measurement equipment and the pumping system. All apparatus are computer driven and the whole acquisition bench has been automated.

1– RF apparatus

The signal delivered by a stable RF generator (20dBm) is amplified using the 5kW klystron. The RF signal is pulsed in order to avoid exessive heating of the cavity. In fact, the cavity is not thermalized (other than by normal air convection) so the duty cycle has been kept lower than 1%. On the other hand, the loaded Q_l beeing $Q_0/2$=4000, the filling time of the cavity is less than 1μs. In order to stay in an established regime, the RF pulses are always longer than 10μs (typically 1ms with a repetition rate of 500ms). Measurements of incident, reflected and transmitted RF power are done with a peak power meter if τ>100μs and with a diode otherwise. A phase locked loop can be used to follow the shift of frequency

and the maximum field in the cavity, but it is also possible to work with an open loop as the bandwidth is large enough to allow manual compensation. In fact, there is only a small and smooth frequency shift due to heating. We choose for mechanical reasons a stainless steel cavity body with a layer of 50μm of copper deposited electrochemically on the surface. Typically, for the maximum power of 5kW in the cavity and a duty cycle of 1%, the outside wall temperature rises from 20°C to 30°C and the frequency decreases by roughly 2MHz.

2– Current emission

One should care about isolating the current collection cable from external perturbation or interferences especially the 50Hz ripple induced by the mains supply. Using a KEITHLEY BNC cable (loaded to reduce FM interference) followed by a current amplifier (KEITHLEY 428) with a gain>10^{10}V/A was the best way to minimize the noise coming from the klystron power supply (50Hz and 300Hz). When not filtering (short pulse lengths, <1ms), our resolution is better than 100pA. With filtering (>1ms), it can be better than 1pA. The maximum current allowed is 10mA. A sample and hold triggered by the pulse generator gives the current at any time during the RF pulse. The output of the current amplifier is also sent to an osilloscope to check the signal response.

3– Pumping system

The pumping system comprises a turbomolecular pump plus a primary Rootes pump, reaching a pressure of 5.10^{-5} mb. Then we switch to a 25l/s ion pump decreasing the pressure to 10^{-8} mb. Corrected for the conductance, the pressure inside the cavity is estimated to be less than 10^{-7} mb. Specific studies of adsorbed gases can be done using a "microleak" valve with a controllable flow rate from gas bottles. Moreover, the whole cavity can be immersed in a Dewar containing liquid nitrogen making it possible to reduce the temperature to 77K.

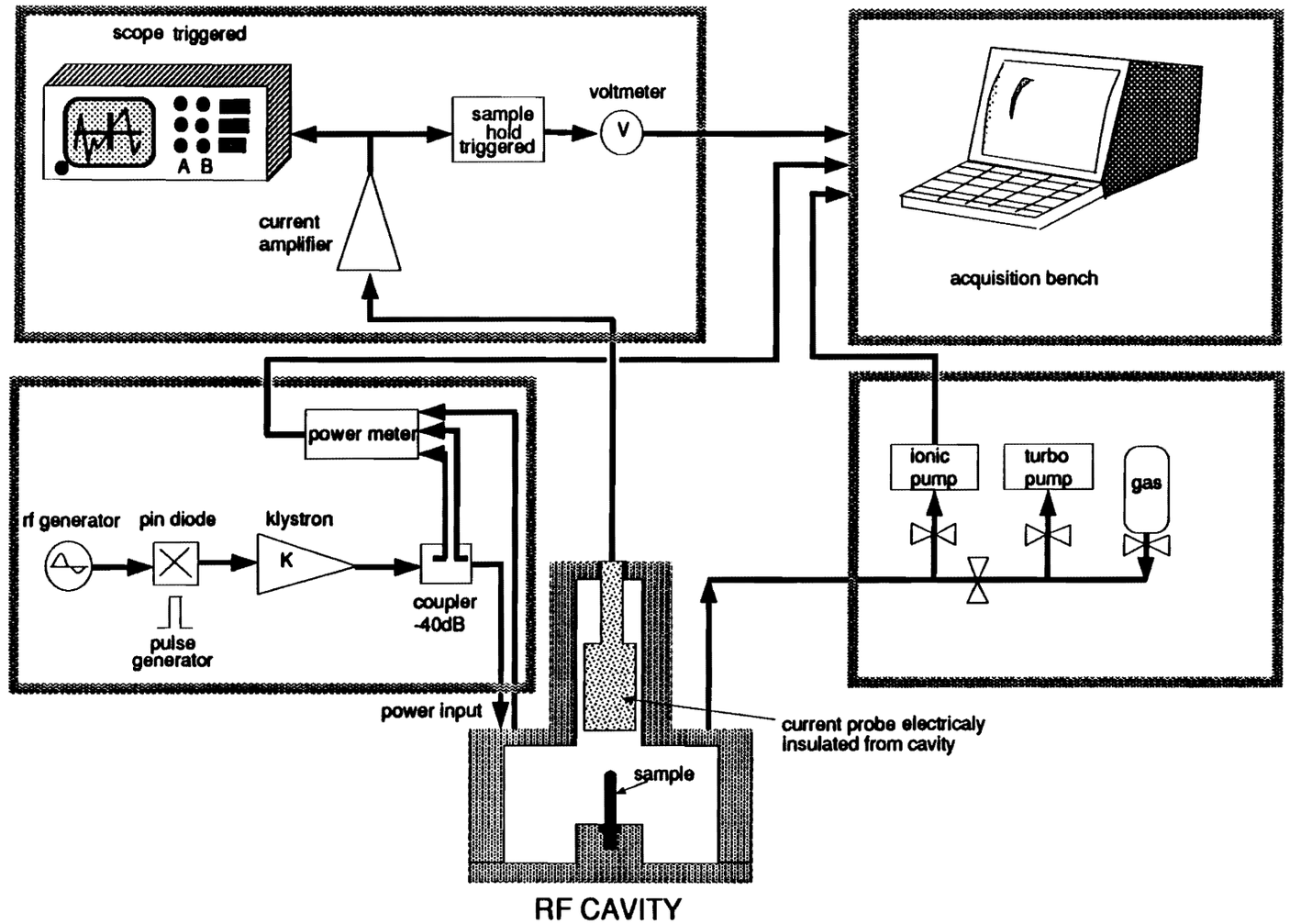

Figure 11– Overall experimental layout

Frequency	1495 ± 5 MHz
Maximum RF power	5 kW
Maximum average power	< 50 W
Maximum peak field (300K)	> 50 MV/m
Maximum peak field (77K)	> 65 MV/m
RF pulse length	10 μs to continuous
Emission current	100 pA to 10 mA
Pressure	< 10^{-7} mb

Table 2– General characteristics of the experiment

IV – First measurements

The first measurements were made on copper and niobium samples. These first observations lead to some remarks about what is really happening inside the cavity. We deduced the specific experimental procedure described below in order to extract the true value of the field emission current.

1– Positive ions

On applying RF power in the cavity, a positive current is often obseved if the vacuum is poor (for example 10^{-5} to 10^{-6} mb). This can be due to either positive ions hitting the probe antenna or electrons leaving it. The hypothesis of positive ions is the more probable one —although the total cross section for ionization is extremely small for the pressure considered [15,16,17] — because it is always accompanied by an increase in the pressure reading. Actually, we observe bursts of pressure synchronised with the RF pulse as long as a positive current is detected on the current antenna. As time passes, there is simultaneously a decrease in the value of the positive ionic current and of the amplitude of the bursts. When the pressure is below 4.10^{-7} mb, the ions disappear and we observe either zero current or a negative field emission current. The field emission current is always remarkably constant as a function of time during the RF pulse. When we try to increase the field, we sometimes

observe spikes of negative current superimposed on the FE current. These spikes appear completely chaotic and of variable amplitude. Their number and amplitude decrease with time and eventually (~15mn) vanish, leaving only the stable FE current which is for us the signature of FE (figure 12).

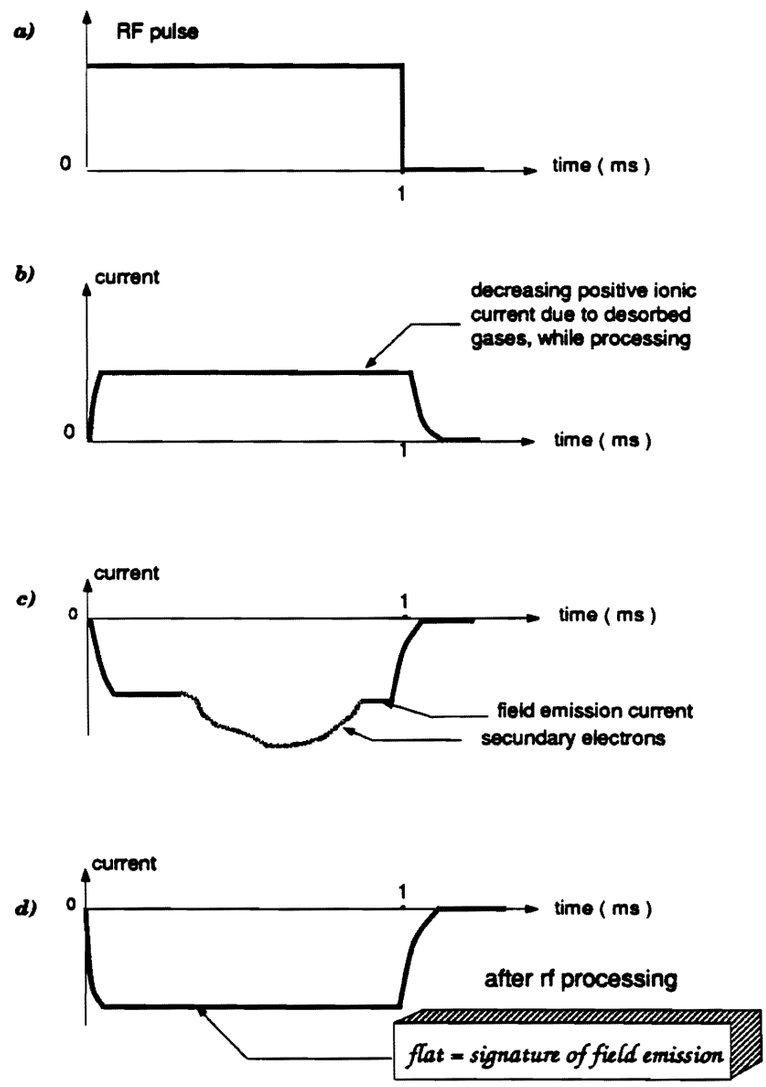

Figure 12– Different scope responses of current as a function of time showing the signature of the real field emission current

This is what we call "forming" the sample. The appearance of positive ions suggests that some kind of discharge occurs inside the cavity between the sample and the antenna. In that region, a high local pressure can give a significant rate of ionization. A short analysis can show that if positive ions are created they will always end up striking the antenna even in an oscillating field and even though they have a heavy mass — contrary to electrons, the ions will need several RF periods to cross the distance separating the sample from the antenna with a back and forth movement getting further each period. Moreover, these ions will strike the antenna with relatively high energies (hundreds of eV, figure 13) where they can cause some damage desorbing gases from the antenna. This desorption will in turn enhance the discharge and that is probably what we observe as a sudden increase of pressure.

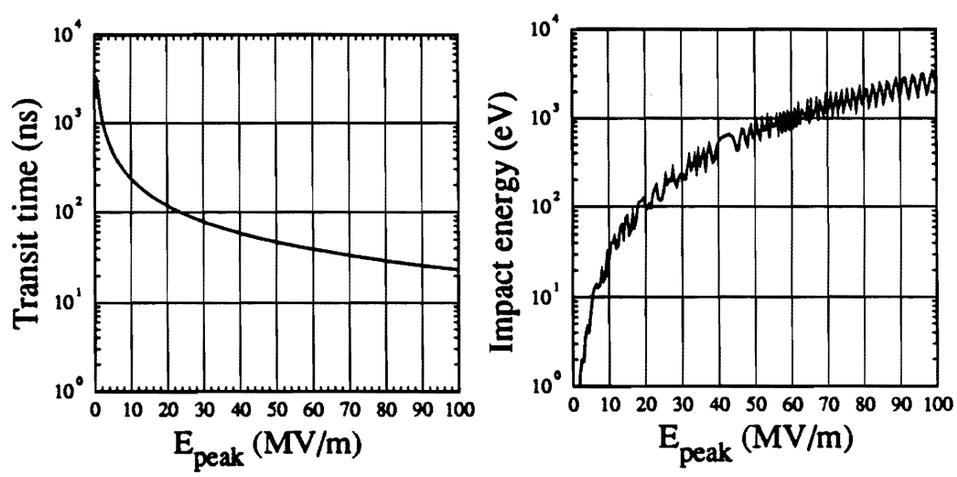

Figure 13– Positive ions transit time and impact energies

2– Adsorbed gases

Adsorbed gases already play an important role in the increase of pressure because when we test again a previously "formed" sample, for example after a couple of days under good vacuum, we once again observe some positive ions although less time is needed to "re-form" the sample. This can be explained by the fact that some gases have had time to re-adsorb on the surface of the antenna or sample even at very low pressure. In any case, it is clear that the phenomenon is not directly related to the fundamental physics of FE as when desorption ends, we always remain with the same FE current as previously measured. Thus these reappearing positive currents do not denote any real modification of the emitter itself.

3– Secondary electrons

We also sometimes observe secondary electrons (SE) either coming from or falling on the probe antenna. They can easily be identified as they can be repelled when we polarize the antenna with a small external continuous voltage (between −5V and +5V) whereas the real FE current does not change at all (we have already seen that the emitted electrons have at least tens of keV). These SE are harmless but can perturb the measurements when they appear. We do not really know why they appear but when they do, the current associated with them can be very high and generally unstable. However, SE generally disappear at very high fields.

4– Multipactoring

Sometimes, at a given field (around 15MV/m), a large current is measured which disappears if we keep going up in field. We associate this with some kind of multipactoring in the ($\lambda/4$) antenna transformer. Electrons collected have there small energies as the field is very low (0.1% of peak field) and the distance from the body of the cavity is less than 0.5mm. We have not concerned ourselves much with the phenomenon, as its occurence is not systematic, and it appears only at fields below those where most sites start to emit.

5– Procedure

Considering all the above described phenomena, we designed a procedure for measuring the "correct" FE current. First, we increase the field slowly, waiting for the desorbed gases to be pumped away and the positive current to disappear. We continue to increase the field to the maximum we can obtain (or wish to use). At this point, we wait for about one half to one hour until the vacuum improves ($<4.10^{-7}$mb). We check that there is no SE or any multipactoring, which is generally the case at high field. Having seen the signature of FE (constant and stable negative current), we can then make measurements as a function of decreasing field. This procedure gives reproducible results for increasing and decreasing fields and seems satisfactory for us as we usually obtain exactly the same curves when measuring the same sample several times even before and after removing and replacing it from the cavity.

6– Fowler-Nordheim analysis

A typical curve obtained with a niobium sample is shown in the next figure. We immediately notice the exponential growth of the current with the electric field which is always the case for a FE current.

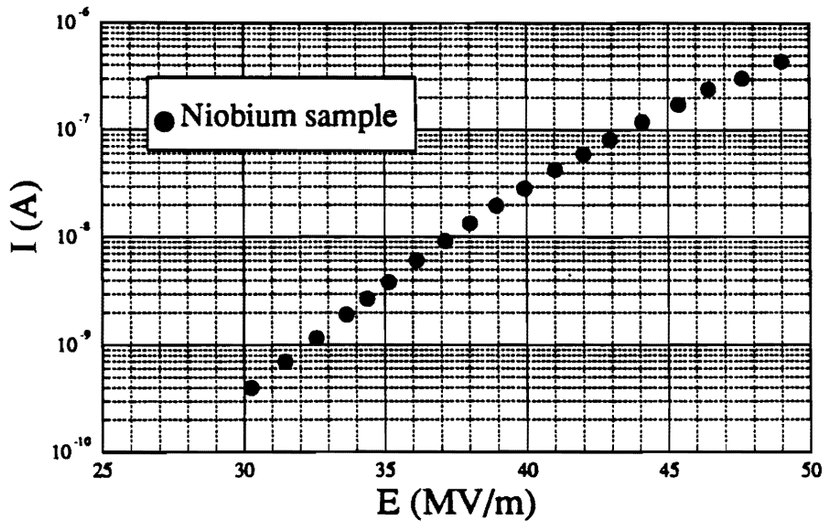

Figure 14– Typical curve of an emitter : detected current as a function of the field

From a Fowler–Nordheim (FN) plot [18] of this data, the so called enhancement factor β and the equivalent emitter surface S can be extracted assuming a given theoretical value for the work function Φ= 4eV for niobium.

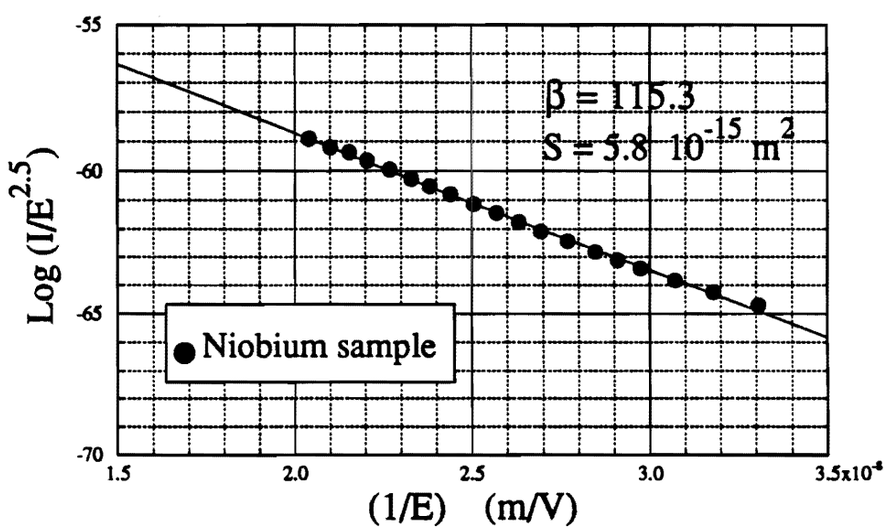

Figure 15– Fowler-Nordheim plot. Enhancement factor β and surface S are extracted from a linear fit.

The analysis in the case of an RF field is done in the appendix justifying the plot of $Log(\frac{I}{E^{5/2}})$ as a function of (1/E) assuming that the basic physics is the same in RF and in DC. The parameter β is inversely proportional the slope of the line while S is given by the ordinate at the origin. All values obtained for β lie between 100 and 200, and for the surface S between $10^{-16}m^2$ and $10^{-13}m^2$.

7– X-Ray measurements

When a high energy electron hits a metal, it may interact with an atome emitting X-rays photons by *bremsshtralung*. The spectrum of X photons can extend from almost zero energy to the maximum possible, which is the energy of the incident electron [19]. The production probability is much greater for low than for high energy X-rays. The number of photons thus decreases with increasing energy and drops to zero exactly at the energy of the incident electron. This phenomenon is useful as it can indicate the presence of FE and give indirect information on the value of the peak field in the cavity. Measurements have been performed using a (75mmx75mm) cylindrical NaI crystal shielded with a 5mm thick sheet of lead. It stands 100mm away from the cavity and is collimated with a diameter of 10mm. Collimation is important in order to avoid piling–up of events. Light emission from the NaI crystal is detected by means of a photomultiplier then analysed with a multichannel analyser similar to those commonly used in nuclear instrumentation (Silena). The whole chain has been calibrated with known X-ray sources Co60, Cs137 and Am231. From each measure, we substract the noise which amount to 30 counts/s for 512 channels almost independent of energy. A typical curve is shown in figure 16. The maximum electron energy is deduced

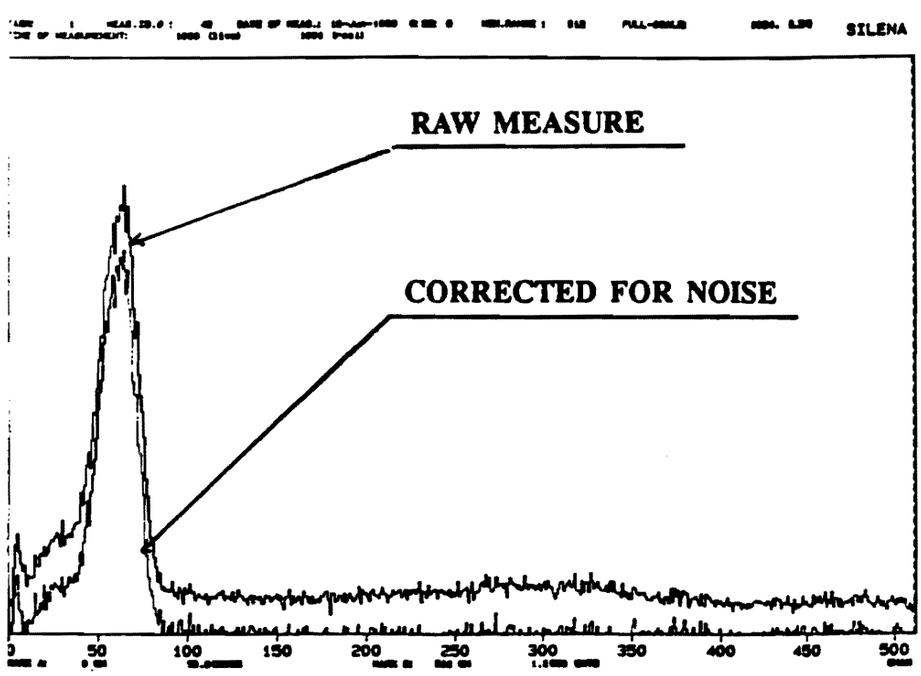

Figure 16– X-ray spectrum. Each channel corresponds to 1.06 keV.

from the maximum X-ray energy detected. These values are plotted (figure 17) along with the energies previously calculated (figure 13). They are very close to the expected energy. This is a further confirmation of the value of the peak electric field in the cavity. The fact that the measured value is 12% above the expected one can be due to two reasons : First, we may have some piling up of events (a few percent) that might artificially widen the spectrum of energy. Secondly, the calculated final energy is obtained using the supposed macroscopic field. But we know the microscopic field is locally enhanced by a factor of $\beta \sim 100$. This could introduce an increase in energy if the enhancement acts over a large enough distance.

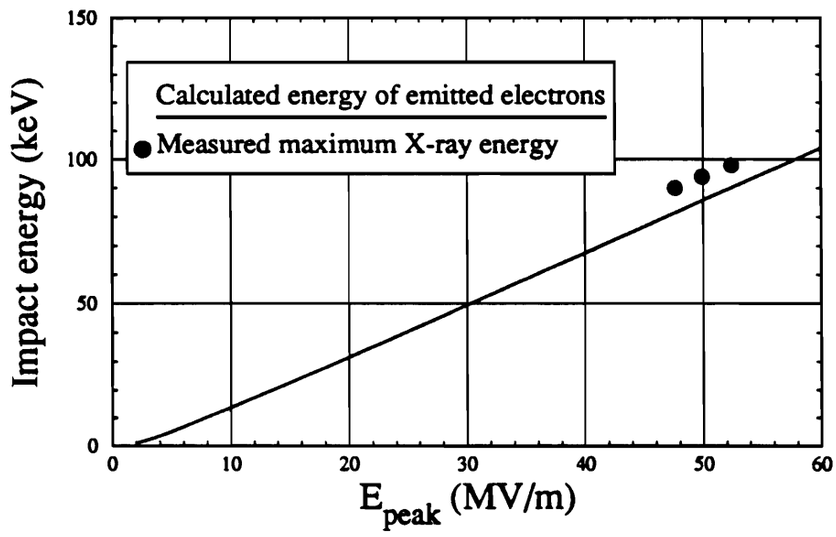

Figure 17– Electron energy as a function of field. The three points show the maximum X-ray energies deduced from three measured spectra.

V – Some results

1– Statistics on "clean" samples

It is known from experience on RF cavities [20] that undesirable FE is minimized if the final treatment is made in a clean room. One is then inclined to conclude that emission is directly correlated with "dust" particles deposited on the surface regions where the electric field is strong. However, we do not know which particles are likely to emit and which not, as even in a class 100 clean room, one gets about 1000 particles per square meter per hour deposited on the surface [21,22]. The main steps in the cleaning procedure followed for all samples are :

— Ultrasonic degreasing for 15mn, rinsing with ultrapure water (resistivity >15MΩ), acid attack (a mix of sulfuric and chromic acid for copper and (1:1:2)HF,HNO_3,H_3PO_4 for niobium).
— Final rinsing with filtered ultrapure water (resistivity>18MΩ), drying in a laminar flow in a class 100 clean room, or in an intermediate class 10000 room.
— Storage of the sample for transportation in a clean closed plastic box.
— Mounting in the cavity under a laminar flow.

Up to now, we have performed 18 tests on niobium samples cleaned following the same procedure and found that 8 of them showed no FE (meaning less than 10pA current) up to 50MV/m. It appears that our treatment leads to a roughly 50% chance of having an emitter occuring on a 0.1 cm^2 area of this kind of niobium surface.

2– Artificial emitters

It is possible to create emitting sites intentionally on a clean surface. We can divide these artificial emitters into two main categories : particles and "intrinsic" emitters [23]. Particles can be deposited by sprinkling on the hemispherical top of the sample powders of different kind of materials (Al_2O_3,SiO_2,Fe,C,Ti,Nb,W,Ta,...) with size between 1μm and 50μm, while intrinsic emitters are made by marking or scratching the surface with a point made of a material harder than the sample (diamond for example). We usually examine the sample using a scanning electron microscope (SEM) before putting it in the RF cavity. After the RF test, it is removed from the cavity and observed again in the SEM, where it is also possible to measure the DC field emission current locally on the site by means of a polarized needle scanning the surface [24]. The full results will be detailed in a forthcoming paper [25]. Main features deduced from these artificial emitters are :

— FE can appear at very low field (5MV/m)
— Some particles disappear generally leaving in their place small craters (5μm) on the surface.
— The particles remaining are lined up along the electric field direction perpendicular to the surface thus maximizing the electric field at their top.
— Their bases are generally melted after the RF test, leaving them well stuck and in good electrical contact with the metal surface.

3– Comparison between cold and warm temperature

We measured the same sample six times, alternating room temperature and liquid nitrogen temperature measurements. The standard FN theory predicts that the influence of temperature on FE should be negligible between 77K and 300K. Suprisingly, we noticed a big difference in the value of the FE current (5 times less) as shown in figure 18, whereas the FN slope β

seems to be the same in both cases (160). We strongly suspect adsorbed gases to be the cause

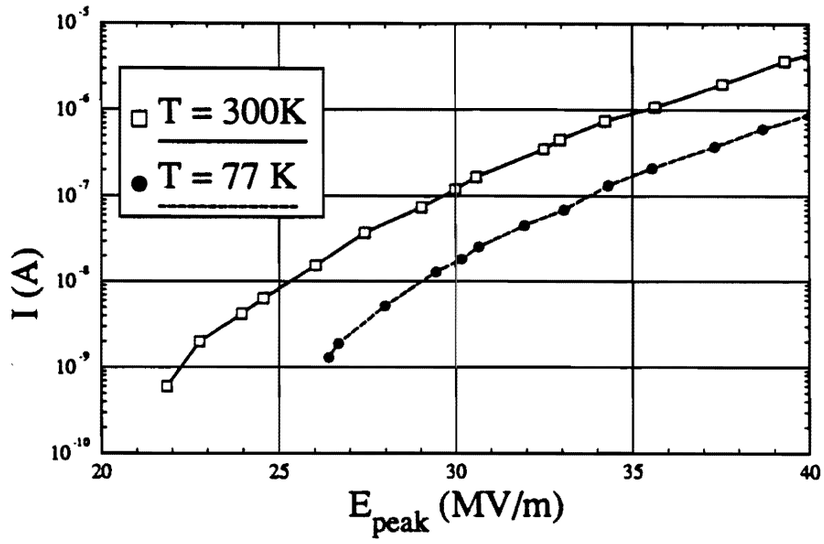

Figure 18– Field emitted current from the same sample at liquid nitrogen (T=77K) temperature and room temperature (T=300K)

of that difference. The explanation could be that layers of external species can reduce the current by modifying the energy barrier between the metal and the vacuum [26,27]. Recent experiments with artificial emitters aiming at comparing DC and RF emission seem to weigh also in favour of this hypothesis [25].

4– Influence of RF pulse length

As thermal effects appear to be of major importance in the mechanism of FE (see the section about artificial emitters), we tried to investigate in the case of dust particle emitters what would happen if we changed the length of the RF pulse. First of all, a quick theoretical estimate shows that the increase in temperature due to RF losses in a particle lying on the surface is at least an order of magnitude higher than that due to Joule losses induced by the emitted current itself. Second, the particles are so tiny that we can assume a steady-state heat flow regime, the transient one being much shorter than the pulse duration. The duty cycle should then have little influence on the FE current. Experimentally, as expected, we do not observe any variation of the current as we shorten the pulse while staying at a constant field. The crucial experiment was realized while contaminating niobium samples with iron particles. We took two samples initially free from FE on which we put hundreds of particles (as counted from the SEM pictures). We tested the samples in the RF cavity using the same duty cycle and increasing to the same level of electric field (45MV/m), but applying to one of them short pulses (200μs) and to the other long ones (10ms). After the RF tests, we took

again pictures with the SEM and counted the remaining particles. On the sample which was tested with the longer pulse, 85% of the particles remained on the surface while only 32% were left on the one tested with the shorter pulse (see figure 19). We repeated the experiment with two other samples and found basically the same result (75% for long pulses, 30% for short). Our conclusion is that short pulses are more effective for "cleaning" the surface of dust particles. This can be understood from the fact that thermal processes are involved : A too long pulse can melt the base of a particle and weld it to the surface more easily than a short pulse. When a particle is welded, it couldn't be removed afterwards anymore. However, if we start with short pulses, the particle will not heat enough to melt and stick to the surface, making it easier for the electrical forces to draw away the particle. Therefore, one must go towards higher fields and shorter RF pulses if one wants to increase the chances of removing emitting particles. This may explain why high peak power processing [28] is so efficient in reducing FE in RF cavities.

LONG PULSE (10 ms)

BEFORE RF TEST

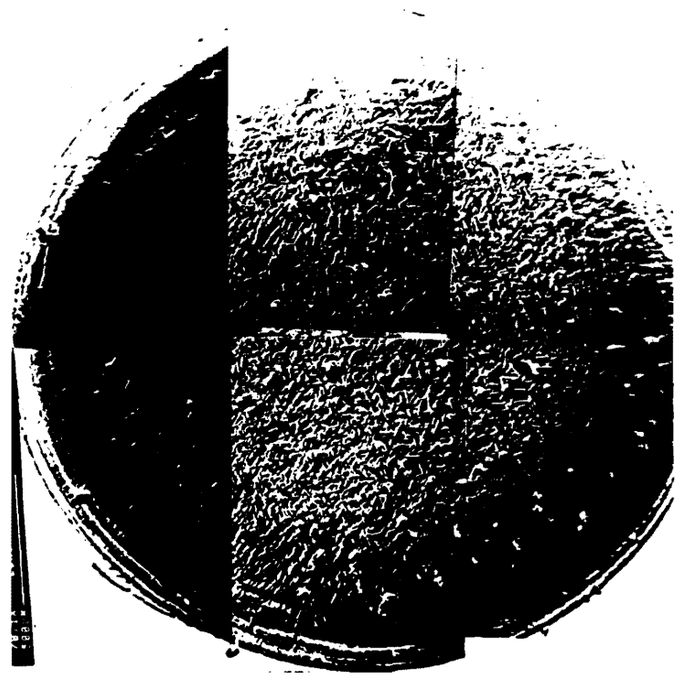

AFTER RF TEST

SHORT PULSE (200 μs)

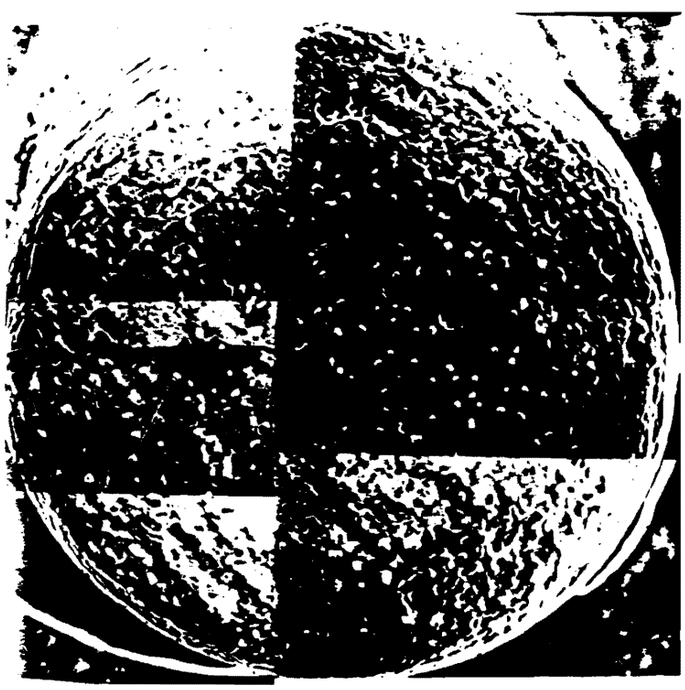

BEFORE RF TEST

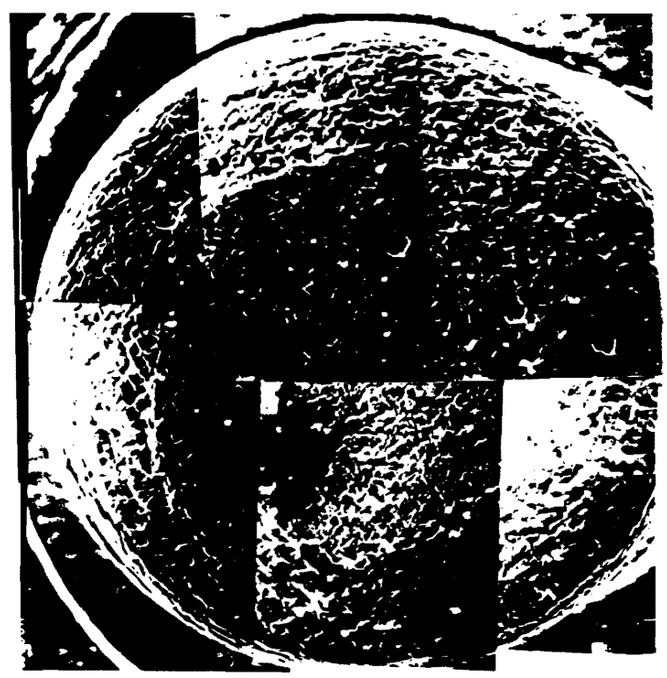

AFTER RF TEST

Figure 19-Pictures showing the number of particles on a niobium sample before and after applying the RF field. Short pulses removed many more particles than longer ones.

5– Various treatments

We have begun to test some samples to determine how specific surface treatments affect FE. We summarize here our observations, bearing in mind that our conclusions will only be definite when enough similary treated samples have been tested —which is not yet the case.

— ***Acid etch :*** We made a standard chemical etch of about 10μm on niobium samples previously contaminated with iron particles. After rinsing with ultrapure water, the samples no longer showed FE (and SEM showed that all particles were removed). We believe that our chemical treatment could reasonably be considered as making a new blank surface on the samples.

— ***Thermal treatment :*** We tried on some other niobium samples a high temperature treatment (above 1800°C for one minute) using an electron beam welding apparatus at Saclay [29]. It is known from earlier studies in DC [30,31] or in RF [32] that heating above 1400°C can remove emitter sites. We took 4 samples which showed FE, heat treated them, then tested them again in the cavity. All four still emitted after the treatment. Only one showed a slightly reduced FE whilst the three others produced exactly the same FE curves. However, further investigation is needed to confirm the result as the samples could have been contaminated during their removal from the electron beam chamber.

— ***Electropolishing :*** This surface treatment is sometimes used for RF cavities to obtain a smooth surface state [33]. We electropolished 4 niobium samples in a chemical bath (hydrofluoric, sulfuric and lactic acid), rinsed them in ultrapure water then tested them in our RF cavity. All four showed "natural" FE. But on three of them, the emission current was much lower than what we usually find for normally etched samples.

— ***Diamond polishing :*** We tested one copper sample which had been diamond polished at LAL (Orsay). It showed no field emission up to an electric field of 63MV/m. Of all the copper samples we tested, it is the only one which could withstand such a high field without emitting. Again, this has to be confirmed on other samples before making a statement.

VI – Future experiments

The first encouraging results of this experiment suggest some improvements that would aid our attempts to understand the physics of FE. First, it seems possible to measure independently the current emitted from the sample by isolating the sample from the body of the cavity. This would enable us to separate the FE current from SE or ion induced currents. Another extension of the experiment would be to visualize *in situ* the emitter sites during exposure to RF and to study any light emitted from them. This can be done by removing the current antenna and replacing it by a sealed sapphire window. A dedicated experiment is under development for that purpose in collaboration with the IPN (Orsay) [34]. Experiments showing how adsorbed gases or special coatings (like SiO_2 for example [35]) affect RF-FE might give interesting

results. One would also like to study the influence of temperatures above 500°C on FE. Ways to heat the sample and to control its temperature are now under investigation.

VII – Conclusion

We have designed and built an apparatus to study RF field emission at a frequency of 1.5GHz. It appears to be a very fine tool that enables rapid measurements up to a field of approximately 70MV/m (large enough for most applications). With a minimum of precautions, any kind of material or surface treatment can be tested in the cavity. The excellent stability and reproducibility of the field emitted current in a radiofrequency field allows one to make precise measurements distinguishing the FE current from other phenomena (ions, secondary electrons, etc...). Initial observations seem to strengthen the geometric hypothesis : the apparent reinforcement of field is merely due to the shape of metallic protrusions on the surface. The old theory of Fowler and Nordheim seems to be sufficient to explain all the data and observations in the cases of "intrinsic" as well as artificial emitters. On the other hand, we have shown that short RF pulses are more likely to "clean" the surface when one deals with dust particles.

Acknowledgments

This work couldn't be achieved without the help and the assistance of all the GECS group at Saclay. We are indebted to G. Leroux for the drawing of the cavity, J.M. Joly and J.M. Poitevin for making the triggered sample and hold, M. Juillard for allowing the use of the perturbation measurement bench, C. Duclos for the X-ray measurements and A. Bouillac for writing the computer acquisition program. We wish to thank Drs G. Muller and U. Klein from Wuppertal University for lending a prototype of $\lambda/4$ resonator and M. Roch from Orsay for preparing the diamond polished sample. Finally, we wish to greatfully thank Dr R. Noer for correcting this paper.

Appendix : Fowler Nordheim plot in RF

One assumes that RF field emission is at anytime what one would obtain with a DC electric field E(t). This hypothesis could be justified by the fact that electrons' time to get out of the metal is probably much lower than the RF period (typically 10^{-15}s as compared to 10^{-10}s). Writing the oscillating electric field on the surface as :

$$E(t) = E_m \, sin(\omega t)$$

and knowing the current law as a function of field $I = f(E)$, one can deduce the emitted current as a function of time.

For simplicity, a fairly good approximation is to replace the curve I=f(E) by its tangent at maximum field E_m as the major contribution to the current occurs when the electric field is close to E_m.

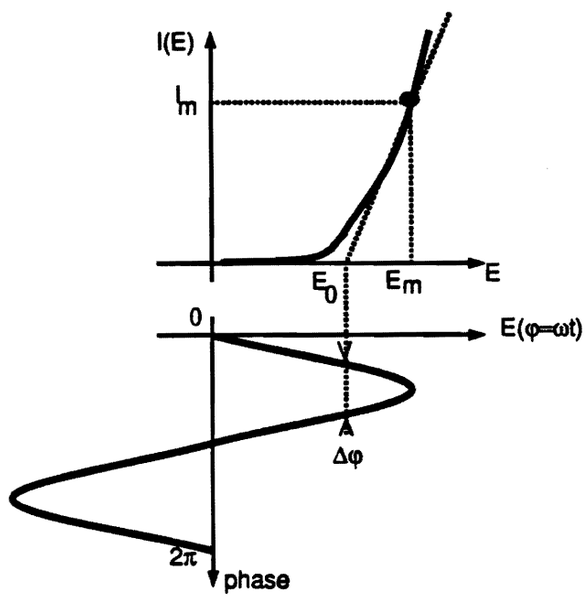

Considering

$$I = I_m + \left(\frac{dI}{dE}\right)_{E=E_m} (E - E_m) = I_m + I'_m \,.(E - E_m)\,,$$

one may calculate the time Δt (and the phase $\Delta\varphi = \omega\Delta t$) over which field emission lasts (see figure):

$$E_m \, cos\left(\frac{\Delta\varphi}{2}\right) = E_m - \frac{I_m}{I'_m}$$

and

$$\Delta\varphi = \sqrt{\frac{8I_m}{E_m I'_m}}$$

The mean current integrated over a RF period is :

$$< I_{RF} > = \frac{1}{2\pi} \int_0^{2\pi} I(\varphi)\, d\varphi = \frac{1}{3\pi} I_m \Delta\varphi = \frac{2\sqrt{2}}{3\pi} \frac{I_m^{3/2}}{\sqrt{E_m I_m}}$$

Now, one can assume a Fowler-Nordheim law for the intantaneous current variation with the electric field, given by [18] :

$$I_m = \alpha\, E_m^2\ e^{-a/E_m}$$

$$with \quad \begin{cases} \alpha = 1.54\ 10^{-6}\ S\, \beta^2/\Phi \\ a = 6.83\ 10^9\ \Phi^{3/2}/\beta \end{cases}$$

Φ being the work function in eV, S the total emitting surface in m^2, β the field enhancement factor characterizing the emitter and E_m the peak field in V/m.

Introducing the preceeding formula into $< I_{RF} >$, one gets the mean current RF field emission as a function of the peak field

$$< I_{RF} > = \frac{2\sqrt{2}}{3\pi}\, \alpha \left(\frac{E_m^{5/2}}{\sqrt{a + 2E_m}} \right) e^{-a/E_m} .$$

There, one may distinguish between two regions :

— $E << a/2$: $I \sim E_m^{2.5}\ e^{-a/E_m}$

— $E >> a/2$: $I \sim E_m^{2}\ e^{-a/E_m}$

For most of our applications one deals with the first case (for example, $\Phi = 4eV$ *and* $\beta = 200$ gives a=273 MV/m).

Usually, by fitting $Y = Log(\frac{I}{E^{2.5}})$ versus X=1/E , one obtains a straight line with negative slope $Y = -aX + b$, the so-called Fowler-Nordheim (FN) plot, the cœfficients being

$$a = 6.83\ 10^9\ \Phi^{3/2}/\beta$$

$$b = Log\left(\frac{2\sqrt{2}}{3\pi} \frac{\alpha}{\sqrt{a}} \right) = Log(\ 4.62\ 10^{-7}\ S\, \beta^2/\Phi\sqrt{a})$$

Inversely, by fitting experimental data, one gets :

$$\begin{cases} \beta = \dfrac{6.83\ 10^9\ \Phi^{3/2}}{a} \\ LogS = 14.5877 - 2\, Log\beta + Log\Phi + \dfrac{1}{2}\, Loga + b \end{cases}$$

References

[1] R.J. NOER, Electron field emission from broad area electrodes, Applied Physics A 28,1–24 (1982)

[2] C. CHIANELLI, A. CURTONI, J. JIMENEZ, J. JODET, A. ZEITOUN-FAKIRIS, G. JOUVE, Electron emission from niobium samples for high applied electric fields, XVth International Symposium on Discharges and Electrical Insulation in Vacuum, Darmstadt, Germany (1992)

[3] C. CHIANELLI & al, 3rd Particle Accelerator Conference, EPAC 92, Berlin, Germany (March 1992)

[4] G.A. LOEW & J.W. WANG, Field emission and RF breakdown in copper linac structures, Particle Accelerators, Vol. 30, p. 225–230 (1990)

[5] E. TANABE, A. Mc EUEN, M. TRAIL, G. MEDDAUGH, S. BANDY, Microwave field emission, Linear Accelerator Conference Proceedings, Chalk River, Canada (1992)

[6] U.KLEIN, J.P. TURNEAURE, Field emission in superconducting cavities, IEEE Trans. on Magn., Vol. MAG-19, N° 3 (May 1983)

[7] MOFFAT & al, Proceedings 4th Workshop on RF Superconductivity, KEK, Tsukuba, Japan (1989)

[8] M.H. COBOURNE & W.T. WILLIAMS, Field emission from superconducting and normal electrodes, Physica 104C, p. 50–55 (1981)

[9] H. HUBNER, First results of a microwave field emission cathode, Optik, 64, N° 2, p. 113–123 (1983)

[10] URMEL is written by U. LAUSTROER, U. VAN RIENEN & T. WEILAND, DESY, Hambourg, Germany

[11] HANSEN & POST, On the measurement of cavity impedance, J. Applied Physics, Vol. 19, N° 11 (Nov. 1948)

[12] W. HAUSER & L. BROWN, Perturbation of waveguides and cavities by spheres and cylinders, J. Applied Physics, 30, p. 1460 (1959)

[13] M. JUILLARD, internal report, GECS/SEA/DAPNIA, C.E. Saclay (1987)

[14] L.C. MAIER & J.C. SLATER, Field strength measurements in resonant cavities, J. Applied Physics, Vol. 23, N° 1 (Jan. 1952)

[15] D. RAPP & al, Total cross sections for ionisation and attachment in gases by electron impact, J. Chemical Physics, Vol. 43, 5, 1464–89 (Sept. 1965)

[16] MASSEY & BURHOP, Electronic and ionic impact phenomena, Oxford

[17] G.A. BOUTRY, *Physique appliquée aux industries du vide et de l'électronique*, Masson Editor, Paris

[18] R.H. FOWLER & L. NORDHEIM, Proceedings Royal Society London A119, p. 173–181 (1928)

[19] HEITLER, The quantum theory of radiation, Oxford, 2nd edition (1944)

[20] Proceedings of the 5th Workshop on RF Superconductivity, D. PROCH editor, Hambourg, Germany (1991)

[21] Handbook of contamination control in microelectronic, Ed. by D.L. TOLLIVER, Noyes publication, New Jersey, USA

[22] SAKATA, Aerosol deposition on wafer surface, 9th ICCS (1988)

[23] MOFFAT & al, Studies of the nature of field emission sites, 5th Workshop on RF Superconductivity, Hambourg, Germany (1991)

[24] M. JIMENEZ, R.J. NOER, G. JOUVE, C. ANTOINE, B. BONIN, J. JODET, Electron field emission from selectively contaminated cathodes, to be published in J. Applied Physics D (1993)

[25] from the authors to be submitted to J. Applied Physics D

[26] A. ZEITOUN-FAKIRIS & B. JUTTNER, J. Applied Physics D, 21, 960–67 (1988)

[27] H.A. SCHEWTTMAN, J.P. TURNEAURE, R.F. WAITES, Evidence for surface state enhanced field emission in RF superconducting cavities, J. Applied Physics, Vol. 45, N° 2 (Feb. 1974)

[28] J. GRABER & al, High peak power RF processing studies of 3 GHz niobium cavities, IEEE Particle Accelerator Conference, San Francisco, USA (1991)

[29] B. BONIN & al, A new surface treatment for niobium superconducting cavities, Conference PAC 93, Washington, USA (1993)

[30] P. NIEDERMAN & al, J. Applied Physics, 59, p. 892 (1986)

[31] E. MAHNER, N. MINATTI, H. PIEL, N. PUPETER, Experiments on enhanced field emission on niobium cathodes, Applied Surface Science 67, 23–28 (1993)

[32] G. MULLER & al, IEEE Trans. Electr. Ins., E 1–24, p. 1013 (1989)

[33] Y. KOJIMA, Proceedings of the 11th International Conference on Cyclotrons and their Applications, Tokyo 86, Japan, KEK preprint 86–67 (1986)

[34] T. JUNQUERA & al, to be presented at the 6th Workshop on RF Superconductivity, CEBAF, Newport News, USA (1993)

[35] D.SUN, P. DATTE, W.W. Mc KAY & F.R. HUSON, Rf breakdown test of SiO_2 coated copper electrodes, IEEE Particle Accelerator Conference 91 , San Francisco, USA (1991)